Build Simul (2024) 17: 1359–1377
https://doi.org/10.1007/s12273-024-1133-6

Effect of solar radiation on human thermal sensation and physiological parameters in a convection–radiation air conditioning environment

Guanyu Li[1], Dong Liu[1] (✉), Anjie Hu[1], Qidong Yan[1], Lina Ma[1], Liu Tang[2,3], Xiaozhou Wu[4], Jun Wang[5], Zhenyu Wang[6]

1. School of Civil Engineering and Architecture, Southwest University of Science and Technology, Mianyang 621010, China
2. Sichuan Province Engineering Technology Research Center of Healthy Human Settlement, Chengdu 610065, China
3. Sichuan University Engineering Design & Research Institute Co. Ltd, Chengdu 610065, China
4. School of Civil Engineering, Dalian University of Technology, Dalian 116081, China
5. College of Architecture and Environment, Sichuan University, Chengdu 610065, China
6. School of Environment and Resources, Southwest University of Science and Technology, Mianyang 621010, China

Abstract

This study focused on the effect of glass structures of modern architecture on the indoor thermal environment during summer. In particular, this study examined how solar radiation significantly altered people's thermal sensations. Laboratory tests on convection–radiation air conditioning systems were conducted, encompassing 12 different scenarios, including diverse indoor open areas, terminal forms, and levels of solar radiation. These tests aimed to explore the physiological and psychological responses of the human body to solar radiation penetrating through windows into the inner room. During the experiments, the participants' subjective thermal sensations and thermal comfort were recorded, along with continuous monitoring of their physiological and environmental parameters. Results showed that solar radiation significantly increased local skin temperature, with a maximum rise of 2.15 °C. Operative temperature is a reliable indicator of human skin temperature and thermal sensation vote (TSV). This study established two models that could predict the skin temperature of individuals indoors through operative temperature under conditions without or with solar radiation, and identified sensitive ranges of operative temperature for both models, to be specific, 26.32 °C to 28.43 °C and 28.51 °C to 34.11 °C, respectively. Furthermore, this study established the relationship between skin temperature and TSV under conditions with and without solar radiation. The results indicate that solar radiation enhances the human body's adaptability to indoor environmental parameters; a convection–radiation system (FC+RF) could be used to optimize indoor thermal control under solar radiation, achieving more stable environmental temperatures and improved indoor comfort.

Keywords

system modeling
solar radiation
mean skin temperature
thermal comfort
terminal form
irradiation area

Article History

Received: 24 January 2024
Revised: 20 March 2024
Accepted: 29 March 2024

1 Introduction

Transparent envelope structure is widely used in modern architecture, and their characteristics significantly influence the thermal efficiency and comfort of buildings. Somasundaram et al. (2020) noted that the thermal transfer properties of glass could lead to significant energy loss, especially under extreme climate conditions. Singh and Garg (2011) discovered that large glass facades might result in excessive solar heat absorption of buildings, increasing cooling loads. Some of the solar radiation entering indoors is reflected and absorbed by interior envelope structures and objects, increasing the temperature of irradiated objects and affecting the indoor thermal environment through convective heat exchange. The influence on the indoor radiation field related to solar radiation (intensity and direction), the relative spatial position between objects, and the surface characteristics of the objects (such as absorptivity and

E-mail: liudong@swust.edu.cn

List of symbols

DBP	diastolic blood pressure (mmHg)
f_p	projected area factor
$F_{i\to j}$	angle factor between the interior surface of the i^{th} enclosure structure and the interior surface of the j^{th} transparent enclosure structure
$F_{S\to i}$	angle factor between the human body and the i^{th} interior surface of the surrounding environment
$F_{S\to j}$	angle factor between the human body and the interior surface of the j^{th} transparent enclosure structure
h_c	convection heat-transfer coefficient (W/(m²·°C))
h_r	radiative heat-transfer coefficient (W/(m²·°C))
I_b	direct solar radiation incident on the subject (W/m²)
I_{bh}	direct solar radiation incident on the floor (W/m²)
I_{dj}	diffuse radiation entering indoors through the j^{th} transparent enclosure structure (W/m²)
N	number of interior surfaces of the enclosure structures involved
N_g	number of glazed surfaces
PR	pulse rate (bpm)
SBP	systolic blood pressure (mmHg)
T_a	air temperature (°C)
T_{mrt}	mean radiant temperature (°C)
T_{op}	operative temperature (°C)
T_i	temperature of the i^{th} interior surface in the surrounding environment (K)
T_{skin}	mean skin temperature (°C)
Z-value	standard test statistic
α_{SW}	human body's absorption rate of shortwave radiation
ε_S	emissivity of the human body
ρ_i	reflectivity of the interior surface of the i^{th} enclosure structure
ρ_{floor}	reflectivity of the floor surface
σ	Stefan–Boltzmann constant, 5.67×10^{-8} W/(m²·K⁴)

Abbreviations

BMI	body mass index
FC	fan coil convection cooling system
FC+RF	convection–radiation cooling systems
PMV	predicted mean vote
RF	radiant floor cooling system
SCV	sudomotor conduction velocity
TCV	thermal comfort vote
TSV	thermal sensation vote

reflectivity) (Marino et al. 2017b). An uneven temperature field that fluctuates with solar radiation changes is formed indoors under the thermal influence of solar radiation. Another portion of the solar radiation entering indoors can directly irradiate the human body in some cases, increasing the skin surface temperature and altering the temperature difference in heat exchange with the surrounding environment, affecting the human thermal balance.

Numerous scholars have studied the thermal environment and comfort under solar radiation (Hodder and Parsons 2007; Marino et al. 2017a; Chaiaypinunt and Khamporn 2021; Huang and Kang 2021; Yi et al. 2022). Hodder and Parsons (2007) and Huang and Kang (2021) considered the influence of solar radiation on indoor thermal environments and its effect on human thermal comfort, a key area in architectural research. A et al. (2022) and Kim et al. (2022) pointed out that solar radiation affects not only the indoor temperature but also the humidity and balance of thermal radiation. La Gennusa et al. (2005) proposed a method for calculating the mean radiant temperature considering the direct and diffuse components of solar radiation. They also developed a method for calculating the mean radiant temperature in the absence of solar radiation or with only diffuse radiation and incorporated the adjusted mean radiant temperature into the PMV equation for thermal environment assessment. Zhou et al.'s (Zhou et al. 2022) study indicated that thermal sensations were higher on the window side due to asymmetric radiation, suggesting that the influence of solar radiation through windows on different indoor areas was significantly varied, and indoor spaces under solar radiation should not be simply considered a uniform entity.

The mechanism of radiative heat transfer can significantly affect the indoor thermal environment, leading researchers to use convection–radiation heating and cooling systems. These systems aim to create a comfortable indoor environment and reduce the influence of solar radiation on indoor conditions by combining convective and radiative heat transfer mechanisms. The studies of Liang et al. (2021) and Xie et al. (2022) showed that the use of radiative heating or cooling could reduce air temperature differences and airflow velocity, enhancing comfort and creating a more uniform indoor thermal environment. Liu et al. (2012) and Vadiee et al. (2019) also supported this finding, with their research emphasizing the effectiveness of radiation systems in heating. These systems can offer a more uniform heat distribution, reduce the movement of dust in the air, and decrease the sensation of drafts, thereby enhancing comfort. Marino et al. (2017a) and Liu et al. (2020) conducted studies on heating in winter, discovering that solar radiation could

reduce the heating load on convection–radiation systems, achieving energy-saving effects. However, research on cooling during summer often remained within the stage of artificial environmental rooms or traditional air conditioning (Pan et al. 2022). Additionally, the area of skin directly exposed to the sun is significantly larger in summer than in winter, and the influence of excessive solar radiation on the physiological and psychological responses of individuals indoors under different air conditioning system forms still requires further investigation.

In recent years, the utilization of physiological parameter changes to reflect human thermal comfort has become a future trend with the rapid development of wearable smart technology. Choi and Yeom (2017) measured skin temperatures at seven selected body parts and developed a decision tree model; the combination of arm, back, and wrist temperatures as inputs yielded the highest accuracy in predicting individual thermal sensations. Operative temperature is an index that integrates the effects of air temperature, mean radiant temperature, and air velocity. This index considers convective and radiative heat transfer mechanisms indoors and is widely used to assess the thermal comfort of indoor environments. Wang et al.'s (Wang et al. 2015) and Fang et al.'s (Fang et al. 2017) research supported this view, and related studies emphasized the importance of correctly understanding and applying operative temperature in designing and maintaining a comfortable and energy-efficient indoor environment (Kolarik et al. 2011; Leung and Ge 2013; Yang et al. 2014). However, few studies have been conducted on the effect of operative temperature on human physiological parameters and psychological reactions. Li et al. (2010, 2019) used sudomotor conduction velocity (SCV) as a temperature-sensitive biomarker to reveal the regulation characteristics of human SCV under different operative temperature ranges in a naturally ventilated environment.

In summary, existing research primarily focuses on indoor thermal conditions under solar radiation or on using solar radiation efficiently in winter to improve human thermal comfort indoors while reducing system energy consumption. However, the study of the physiological and psychological responses of solar radiation on the indoor human body under convection–radiation systems during summer cooling conditions still needs to be further explored. In this study, a detailed investigation was conducted on the characteristics of human physiological and psychological responses involving different indoor irradiation areas, terminal forms, and solar exposure conditions in a laboratory equipped with convection–radiation cooling systems. After confirming that operative temperature is a reliable indicator effectively reflecting human skin temperature and thermal sensation vote (TSV), this study further established models to predict the skin temperature of individuals indoors through operative temperature under conditions with or without solar radiation. The findings of this study provide significant experimental evidence for the design and operation of indoor air conditioning systems in summer, with the potential to enhance indoor thermal comfort and energy efficiency.

2 Methodology

2.1 Laboratory introduction

The above-mentioned laboratory is located on the fifth floor of a multifunctional office building in Mianyang City, Sichuan Province. Mianyang City is situated in a subtropical humid monsoon climate zone and is classified as a hot summer and cold winter region in China's architectural climate zoning. The summer in this area is characterized by high temperatures and heavy rainfall, with average temperatures ranging between 29 °C and 32 °C and average relative humidity between 60% and 70% (Atlas Weather 2023). In view of these climatic characteristics, especially the intense heat and the obvious decrease in comfort during summer, the need for an effective cooling system in the region is extremely urgent. Therefore, in order to ensure the accuracy and usefulness of the data obtained, the time period that best matched the local climatic conditions, i.e., 2:30 PM to 4:30 PM, was chosen for this experiment, and all the experimental days were scheduled to be carried out between the end of June and the beginning of August.

The laboratory has a floor area of 60.34 m^2, a building height of 3.2 m, and a ceiling height of 2.7 m. The room's outer wall faces west and has a heat transfer coefficient of 0.84 W/(m^2·K).

The external windows are equipped with standard double-glazed tempered glass (6+12A+6), with a heat transfer coefficient of 3.30 W/(m^2·K), covering an area of 19.3 m^2. The window-to-wall ratio is 80%, with an external visible light transmittance of 0.75 and a near-infrared transmittance of 0.25. The east-facing interior wall near the corridor has a heat transfer coefficient of 1.57 W/(m^2·K). The floor is made of wooden material, with an approximate surface reflectivity of 0.4. The positioning of the laboratory participants, area division, and layout of measurement points can be seen in Figure 1.

The experiment utilizes a combined convection–radiation cooling system powered by an air source heat pump as the main unit. The system comprises a cold source, convective terminal, radiative terminal, thermal storage water tank, manifold, primary water pump, and secondary water pump, among others. The specific configurations are as follows: The

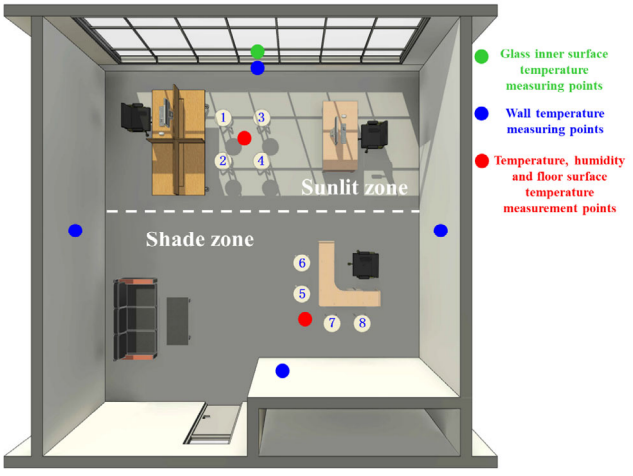

Fig. 1 Layout of the experimental participants positions, area divisions, and measurement points

cold-and-heat source is a household air source heat pump unit (YVAG012RSE), with a rated cooling capacity of 11.2 kW and cooling input power of 3.8 kW; the convective terminal consists of two fan coil units (TBFL-56), each with a rated cooling capacity of 5.6 kW, they are installed symmetrically in the room near the east wall at a height of 2.5 m above the floor and positioned along the centerline of the room to ensure optimal air circulation and temperature distribution; the radiative terminal is a floor radiation system using prefabricated dry modules, with floor pipes of 10 mm diameter PE-Xb in a spiral serpentine layout, spaced 90 mm apart. Images of the laboratory setup, test subjects, and the structure of the radiative terminal can be found in Figures 2(a)–2(c). Additionally, a total heat recovery fresh air exchanger (YRAR003F000RA) was installed to ensure the minimum required fresh air volume indoors, with a rated airflow of 300 m^3/h and an input power of 219 W. In the experiment, the host water supply temperature is set to 7 °C, the fan coiler air supply volume is set to 1020 m^3/h, and at the same time, the indoor temperature is used as the temperature control index of the system, and the thermostat for this experiment is set to 26 °C, and the fan coils and radiant terminals of the experiment are equipped with independent thermostats, which allow the temperature to be set for each terminals; when the temperature drops below the predetermined level, the equipment will restart.

2.2 Information on the test subjects

In order to determine an appropriate sample size, we used a general approach based on statistical efficacy analysis (Choi 1997) in this study. This method was initially introduced into human experiments from social statistics by Lan and Lian (2010) and was applied in subsequent studies by Wu et al. (2019) and Pan et al. (2022).

Various thermal comfort studies have indicated that temperature has a significant effect on human thermal responses; thus, its effect size is considered to be medium or large. This work utilized G*Power 3.1 software for these statistical analyses. In this experimental study, the test type was set as an *F*-test, and the effect size was taken as 0.4 based on the effect size reference values provided by Cohen (1992), with the α significance level set at 0.05, statistical power $(1-\beta)$ at 0.8, sphericity assumed correction factor at 0.5, and the correlation coefficient for repeated measures at 0.5. We calculated that the necessary sample size is 12 people, based on these parameters. To minimize errors and align with previous research recommendations (Lei et al. 2023), the experimental sample size should exceed the minimum required sample size by at least 3 participants. Therefore, we ultimately recruited 16 participants, comprising 8 males and 8 females. All participants are undergraduates or postgraduates from Southwest University of Science and Technology, and they were evenly distributed into the experiment according to their free time. Written informed consents were received from all participants.

Table 1 summarizes the personal information of all participants, all of whom maintained good health during the experiment, with no symptoms, such as colds or fever. Additionally, all participants had resided in Mianyang for at least 1 year, having adapted to the local climate, to minimize the influence of their thermal history on the experimental results. Prior to the experiment, all participants were required to ensure sufficient sleep and avoid alcohol and coffee within 24 h. All precautions during the experiment

Fig. 2 Laboratory introduction: (a) photo of the laboratory, (b) test image of the subjects, (c) diagram of the radiation terminal structure

Table 1 Information of the test subjects

Gender	Age (years)	Height (cm)	Weight (kg)	BMI (kg/m^2)
Male	22.7±3.5	175.2±2.35	66.20±9.68	21.56±3.07
Female	20.7±2.3	162.4±5.18	53.67±7.02	20.32±2.33
Average	21.7±3.0	168.8±3.77	59.94±8.35	20.94±2.70

Note: BMI stands for body mass index.

were agreed upon by the participants, and they were allowed to interrupt the experiment at any time if they felt discomfort.

During the experiment, all participants were required to dress in typical summer attire: wearing short-sleeved T-shirts and shorts (extending to the upper thigh), donning ankle-high socks, and wearing sports shoes. The participants were seated on backless chairs, which had a contact area against the human body of approximately 0.6 m^2, to simulate a common indoor environment in summer. In the assumptions of this study, the insulating properties of the chairs were not considered. The thermal resistance of the clothing worn by the participants was calculated to be approximately 0.5 clo based on these conditions.

2.3 Data measurement

2.3.1 Collection of environmental parameters

This study deployed temperature and humidity sensors in two specific areas, namely, the sunlit and shade zones, to precisely measure the indoor environmental parameters. These probes were positioned at a height of 1.1 m, corresponding to the head height of the seated individuals, to ensure that the collected data accurately reflected the temperature conditions of the environment where the research assistants were situated. Thermocouples were specifically attached to the inner surface of the enclosure structure, the floor of the sunlit zone (Figure 1 sunlit zone), the floor of the shade zone (Figure 1 shade zone), and near the windows to study the influence of solar radiation on the different indoor areas. Shading measures were also taken to prevent the probes from being directly exposed to solar radiation. Additionally, a solar radiation recorder was placed outdoors in an adjacent room to record solar radiation intensity, with its data representing the solar radiation intensity experienced by participants in the sunlit zone during the experiment. The specific locations of these sensors can be seen in Figure 1. All temperature, humidity data, and wind speed information were collected by the corresponding temperature–humidity sensors and anemometer and automatically saved into a computer via the convection–radiation systems monitoring software we had previously developed (Liu et al. 2022b; Liu et al. 2023).

The various measuring instruments used in this experiment, along with their ranges and accuracies, are detailed in Table 2, all conformed to the ISO-7726 standard (ISO 2002). The measurements of all instruments fell within the range corresponding to their accuracy.

The mean radiant temperature (T_{mrt}) is defined as the uniform temperature in a hypothetical environment where the radiant heat transfer from the human body is equal to that in the actual environment. In a uniform environment, the contribution of T_{mrt} to comfort is typically similar to that of air temperature (Fanger 1970), or slightly less (McNall 1968). McIntyre and Griffiths (1972) noted that the proportions of effects between radiant and convective heat transfer were approximately 0.44 and 0.56, respectively. Different surfaces have varying responses to shortwave or longwave radiation, affecting the relative significance of radiation and convection. In particular, shortwave radiation typically originates from small-area sources with high emission temperatures and strong directivity, such as solar radiation. Solar radiation, including direct and diffuse radiation, significantly affects the indoor radiation field and is a major cause of indoor discomfort (Marino et al.

Table 2 Measured parameters in the experiment

Measured parameters	Instrument name	Instrument model	Range	Accuracy
Air temperature	Temperature and humidity sensor	RS-WS-N01-2	−40 °C to 80 °C	±0.3 °C
Relative humidity			0%–100% RH	±2% RH
Air velocity	Air velocity sensor	WD4122	0–5 m/s	±0.02 m/s
Solar radiation intensity	Solar radiation recorder	RS-TBQ-N01-AL	0–2000 W/m^2	< 8 W/m^2
Building envelope inner surface temperature	Temperature sensor	TH10S-B	−40 °C to 80 °C	±0.5 °C
Skin temperature	T-type thermocouple	TT-T-36-SLE	−40 °C to 125 °C	±0.5 °C or ±0.4%
Blood pressure	Electronic blood pressure monitor	EW-BW33	90–250 mmHg (systolic) and 60–180 mmHg (diastolic)	±3 mmHg
Pulse rate (PR)			30–160 bpm	±5%

2015; La Gennusa et al. 2007). Accordingly, the influence of solar radiation must be separately considered when assessing the indoor environment. The manner that solar radiation types enter the indoor environment through windows and their exchange with the human body differ due to their different characteristics, which require separate treatment (La Gennusa et al. 2007). Moreover, previous calculations of T_{mrt} under solar radiation rarely considered the phenomenon of floor reflection (Pan et al. 2022; Song et al. 2022; Ji et al. 2024; Liu et al. 2024), resulting in an underestimation of T_{mrt}. This work refines these calculations based on Marino's research (Marino et al. 2017b). T_{mrt} can be calculated using Equation (1) when solar radiation is not considered. When considering the influence of solar radiation, Equation (2) should be used, which requires knowledge of the temperature of the interior surfaces of the enclosure structure, their position relative to the human body, and the amount of direct and diffuse solar radiation. The mean radiant temperature is calculated using Equations (1) and (2):

$$T_{mrt} = \sqrt[4]{\sum_{i=1}^{N} F_{S\to i} T_i^4} - 273.15 \tag{1}$$

$$T_{mrt} = \left\{ \sum_{i=1}^{N} F_{S\to i} T_i^4 + \frac{\alpha_{SW}}{\varepsilon_S \sigma} \left[\sum_{j=1}^{N_g} F_{S\to j} I_{dj} + f_p I_b + \sum_{i=1}^{N} \rho_i \left(\sum_{j=1}^{N_g} F_{i\to j} I_{dj} \right) F_{S\to j} + 0.5 \rho_{floor} I_{bh} \right] \right\}^{1/4} - 273.15 \tag{2}$$

where T_{mrt} is the mean radiant temperature (°C), $F_{S\to i}$ is the angle factor between the human body and the i^{th} interior surface of the surrounding environment, T_i is the temperature of the i^{th} interior surface in the surrounding environment (K), α_{SW} is the human body's absorption rate of shortwave radiation, ε_S is the emissivity of the human body, σ is the Stefan–Boltzmann constant that equals to 5.67×10^{-8} W/(m^2·K^4), N_g is the number of transparent enclosure structures, $F_{S\to j}$ is the angle factor between the human body and the interior surface of the j^{th} transparent enclosure structure, I_{dj} is the diffuse radiation entering indoors through the j^{th} transparent enclosure structure (W/m^2), f_p is the projected area factor, I_b is the direct solar radiation incident on the subject (W/m^2), N is the number of interior surfaces of the enclosure structures involved, ρ_i is the reflectivity of the interior surface of the i^{th} enclosure structure, $F_{i\to j}$ is the angle factor between the interior surface of the i^{th} enclosure structure and the interior surface of the j^{th} transparent enclosure structure, ρ_{floor} is the reflectivity of the floor surface, and I_{bh} is the direct radiation incident on the floor (W/m^2).

The operative temperature (T_{op}) considers convective and radiative heat exchange between the environment and the human body. When the environmental temperature is close to the comfort range, T_a and T_{mrt} have a significant influence on human thermal sensation. In natural environments, various environmental parameters interact with each other. Research on the influence of a single environmental parameter on human thermal sensation is not feasible. Accordingly, T_{op} is selected as a comprehensive index to study the influence of environmental parameters on human thermal sensation. The operative temperature is calculated using Equation (3) (Li et al. 2021):

$$T_{op} = \frac{h_r T_{mrt} + h_c T_a}{h_r + h_c} \tag{3}$$

where T_{op} is the operative temperature (°C), h_r is the radiative heat transfer coefficient (W/(m^2·°C)), h_c is the convection heat transfer coefficient (W/(m^2·°C)), and T_a is the air temperature surrounding the human body (°C).

2.3.2 *Physiological parameters*

In this study, the physiological parameters of focus included skin temperature, blood pressure, and heart rate. Skin temperature was measured using T-type thermocouples, with data recorded every 5 min. Blood pressure and heart rate measurements were assisted by research assistants using contact instruments, coinciding with the timing of questionnaire responses. Detailed information about these devices can be found in Table 2. The calculation of the mean skin temperature (T_{skin}) used the six-point method, in accordance with the study by La Gennusa et al. (2005). The specific calculation formula is provided in Equation (4).

$$T_{skin} = 0.07T_{forehead} + 0.175T_{chest} + 0.175T_{back} + 0.05T_{hand} + 0.14T_{upperarm} + 0.39T_{thigh} \tag{4}$$

Considering the potential differing influences of solar radiation on both sides of the human limbs, the measurement points were set on the left and right sides of the upper arms, backs of the hands, and thighs. Accordingly, the local skin temperature of nine body parts was measured in this experiment, with the temperatures of the upper arm, back of hand, and thigh averaged between the left and right sides for calculation. The specific locations of each measurement point are shown in Figure 3.

2.4 Questionnaire

In this experiment, two forms of questionnaires were used: paper and electronic. The paper questionnaire was primarily

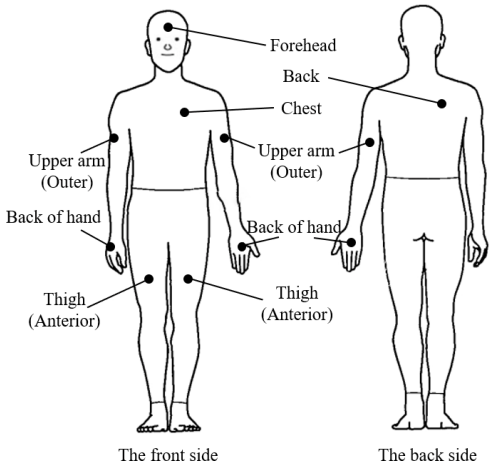

Fig. 3 Layout of the human body skin temperature measurement points

used to collect basic sociodemographic characteristics and some physiological data of the participants, including gender, age, height, weight, blood pressure, and heart rate. Blood pressure and heart rate data were recorded by the research assistants, while the rest of the information was filled out by the participants themselves before the start of the experiment. The electronic questionnaire was used to collect the participants' subjective assessments of the indoor environment. We used a seven-point continuous scale (Wang et al. 2015; Pan et al. 2022) from the ASHRAE-55 standard to assess the participants' overall and local (including forehead, chest, back, upper arm, back of hand, thigh, calf, and foot) TSV. The scale ranges from "cold" (−3) to "hot" (+3), in the following order: cold (−3), cool (−2), slightly cool (−1), neutral (0), slightly warm (+1), warm (+2), and hot (+3). Thermal comfort vote (TCV) was assessed using a four-point scale (Djongyang et al. 2010), including the following levels: neutral or comfortable (0), slightly uncomfortable (−1), uncomfortable (−2), and very uncomfortable (−3). The related rating scales are detailed in Table 3.

Table 3 Subjective vote scale

Scale	TSV	TCV
3	Hot	—
2	Warm	—
1	Slightly warm	—
0	Neutral	Comfortable
−1	Slightly cool	Slightly uncomfortable
−2	Cool	Uncomfortable
−3	Cold	Very uncomfortable

2.5 Experimental procedure

The participants were divided into groups of 16 based on their free time schedules, maintaining a 1:1 male-to-female ratio. At the beginning of each experimental day, eight participants were randomly assigned to various seating positions to ensure a balanced gender ratio in each area. To minimize the influence of shadows cast by desks on the experiment, the research assistants guided the participants to slightly adjust their positions and postures to ensure that the major lower body parts (thighs, calves, and ankles) were not obscured.

In the present study, we asked all participants to sit facing the window on the right side, which was done based on several important considerations. First, this ensured that participants received uniform visual information (Mollon et al. 2017), reducing variability due to differences in location or facing, and increasing the reliability of the results. Second, uniform experimental conditions were essential for controlling variables, ensuring that environmental factors had the same effect on each participant (the exact location is shown in Figure 1). Finally, considering that body orientation may affect the psychological and physiological state of participants (Golmohammadi et al. 2021), uniform orientation helps eliminate directional bias, ensuring consistency and comparability of data. At the same time, this arrangement meant that the right side of the skin of those sitting near the window was usually exposed to more radiation than the left side.

The participants were required to arrive at the laboratory 30 min before the start of the experiment to ensure the accuracy of the experiment. This initiative was carried out to eliminate any influence of their environment or activities prior to arrival on the experimental results. During this time, the research assistants checked if the participants' clothing met the experimental requirements, assisted them in attaching the skin temperature thermocouples, and trained them in using the blood pressure monitors. The research assistants also explained to the participants the precautions to be taken during the experiment, such as the sensations represented by each quantified value and the postures to be maintained. The specific experimental procedure is shown in Figure 4.

After considering the orientation of the laboratory and conclusions from previous studies (Liu et al. 2022a; Liu et al. 2022b; Liu et al. 2023), the study decided to set the experiment time from 2:30 PM to 4:30 PM. The intensity of outdoor solar radiation was relatively stable and high, remaining above 300 W/m^2 for a long time. Considering that summer indoor environments typically required dehumidification through the convective terminal, this experiment investigated two terminal forms: convection–radiation cooling systems (FC+RF) and fan coil convection cooling system (FC).

To minimize the effects of solar radiation through the

west-facing windows under certain cases, a double layer of blackout fabric with a silver coating on the inner side of the west window curtains was added, achieving a reflectivity of 0.9. Under the experimental conditions with the curtains closed, this helped to significantly minimize the impact of solar radiation on the indoor environment. This study designed six sets of experimental conditions to investigate the thermal comfort of individuals with different terminal forms and in various indoor partition scenarios based on these setups. This study also conducted an additional six sets of experiments to further investigate the influence of solar radiation. The experimental conditions are detailed in Table 4.

2.6 Statistical analysis

Data preprocessing was considered a key step in ensuring the correctness of the analysis results in this study.

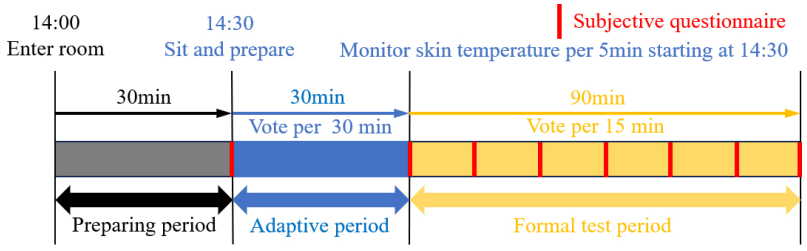

Fig. 4 Experimental flow chart

Table 4 Description of cases

Case	Terminal form	Partition: Sunlit zone	Partition: Shade zone	Solar radiation	Schematic
1	FC+RF	ON	ON	OFF	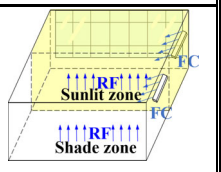
2	FC+RF	ON	OFF	OFF	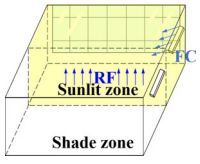
3	FC+RF	OFF	ON	OFF	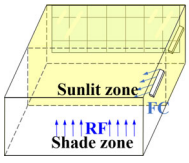
4	FC	ON	ON	OFF	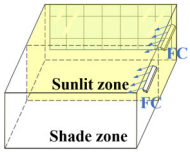
5	FC	ON	OFF	OFF	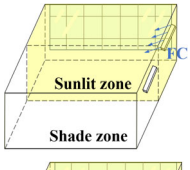
6	FC	OFF	ON	OFF	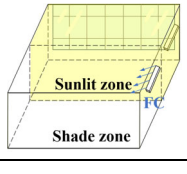
7	FC+RF	ON	ON	ON	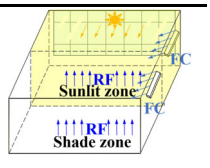
8	FC+RF	ON	OFF	ON	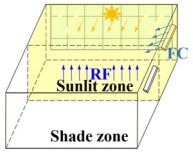
9	FC+RF	OFF	ON	ON	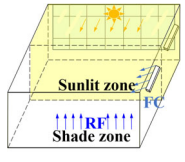
10	FC	ON	ON	ON	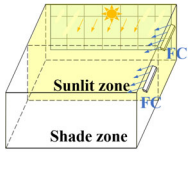
11	FC	ON	OFF	ON	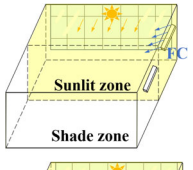
12	FC	OFF	ON	ON	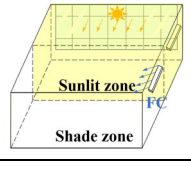

Standardized testing instruments were used to measure the environmental and human physiological parameters. These instruments were rigorously calibrated and verified before the start of the experiment. Furthermore, the participants involved in the testing were trained on how to use the blood pressure and heart rate monitors to ensure the reliability of the data. During the data preprocessing stage, the Kolmogorov–Smirnov (K–S) test was used to verify whether the data followed a normal distribution, which was fundamental in choosing the appropriate statistical methods. *Z*-score normalization was used on the data that followed a normal distribution to remove outliers. Meanwhile, the box plot method was employed for the data that did not follow a normal distribution to exclude outliers. Considering that the intervals of experimental parameter measurements might vary, this study ensured the consistency between the parameters and the questionnaire records by setting the appropriate data collection times to ensure that the collected data could be used as a basis for analysis. Given that the experiment was conducted in different environments, it became necessary to smoothen and discretize data, such as temperature. The BIN method and the minimum information entropy algorithm were used to process continuous temperature data. The minimum information entropy algorithm, based on the principle of minimizing information (entropy), was used to find the optimal data partition intervals and ranges to achieve reasonable discretization results.

After processing with SPSS 27 software, the lowest and highest temperatures of the sample, as well as the optimal number and size of data segmentation intervals, were determined. When conducting variance analysis and hypothesis testing, the normal distribution of the data and the equality of variances were first considered. Methods, such as independent samples *t*-test, paired samples *t*-test, one-way ANOVA, Wilcoxon signed-rank test, and Kruskal–Wallis test, were selected depending on the characteristics of the data. Pearson and Spearman correlation analyses were used in assessing the correlation between data groups. Pearson analysis is applicable to the data sets that conform to a normal distribution and satisfy linear relationships, while Spearman analysis is suitable for the data that do not meet these criteria. Linear and logistic regressions were also used to explore the relationships between specific variables. All statistical analyses were completed in SPSS 27 software, and the specific markers were used in this study to indicate different levels of significance. For example, results significant at the 0.01 level were marked as **, and those significant at the 0.05 level were marked as *.

3 Results

3.1 Influence of environmental parameters on TSV

The correlation between overall thermal sensation and indoor environmental parameters is presented in Table 5, excluding outdoor solar radiation. The results indicate a significant positive relationship between overall thermal sensation and T_a, T_{mrt}, and T_{op} (correlation coefficient > 0.7). A negative relationship with indoor relative humidity could also be observed, but no correlation was found with indoor air velocity. This result suggests that various temperature parameters remain the primary influencers of thermal comfort for individuals in indoor spaces.

Given that correlation analysis did not reflect the distribution of parameters, an analysis of the concentrated evaluation of the overall thermal sensation (−1 to +3) during the experiment was conducted. Box plots in Figure 5 depict the range of several environmental parameters in relation to the overall thermal sensation.

Experiment feedback showed thermal sensation scores ranging from −1 to 3. Figure 5's box plots illustrate the relationship between these scores and environmental conditions. K-W tests on three parameters indicated that air temperature differences significantly affected thermal sensation at lower, but not higher, temperatures. The influence of the three temperature parameters on thermal sensation increased with the standard test statistic *Z*-value, with the *Z*-value of T_{op} being the most significant. Therefore, it is better that operative temperature be used as the primary driving factor for thermal sensation.

3.2 Influence of the different terminal forms on TSV

This section compares and analyzes the thermal comfort of FC and (FC+RF) under summer conditions. It explored the influence of these two systems on the comfort levels of indoor occupants, taking into account the divergent heat transfer mechanisms and the associated requirements for dehumidification. Figure 6 shows the human body's thermal sensation changes. The study analyzed Cases 1–6 to see how different systems influence summer indoor comfort.

Table 5 Correlation analysis between thermal sensation and environmental parameters

	Air temperature	Mean radiant temperature	Operative temperature	Relative humidity	Air velocity
Spearman ρ	0.756**	0.762**	0.781**	−0.209*	0.001

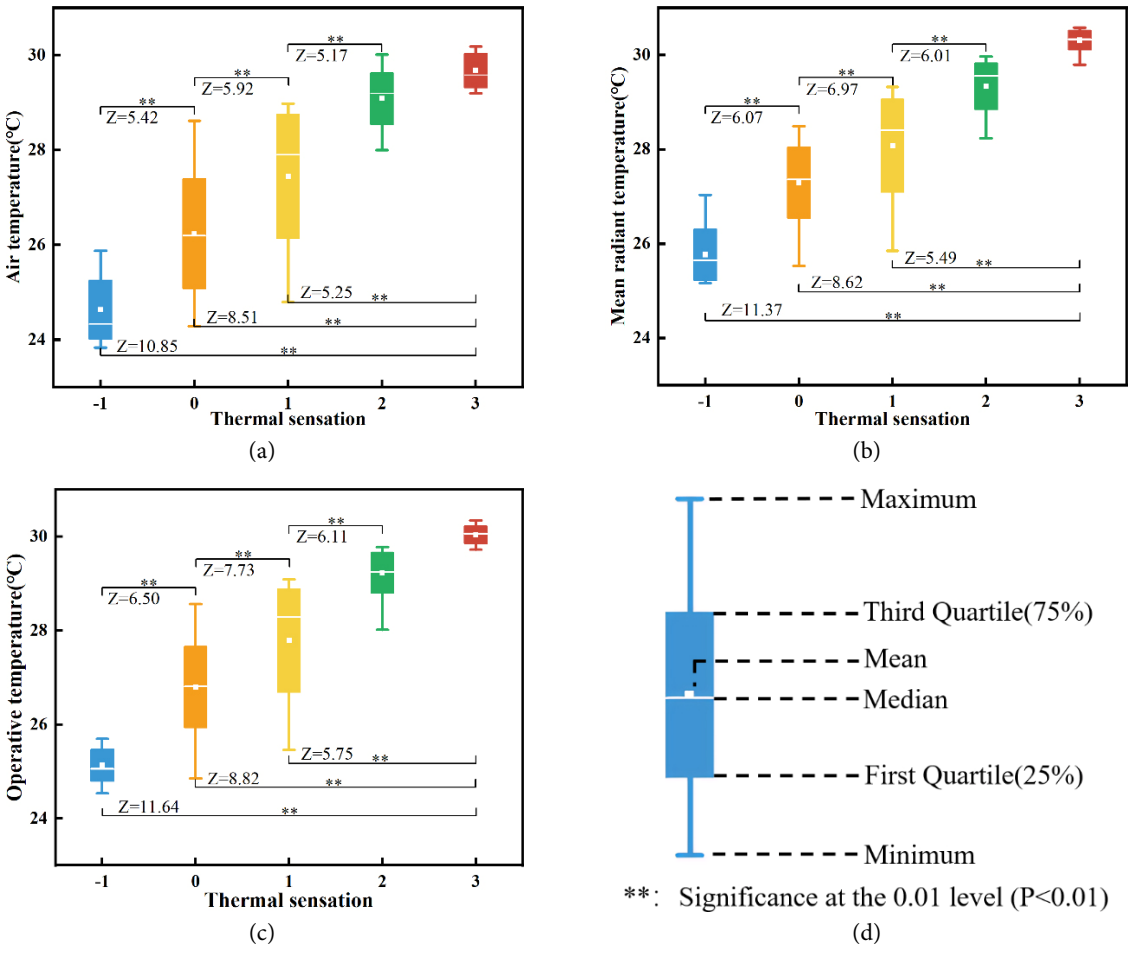

Fig. 5 Interval diagram of the environmental parameters relative to overall thermal sensation: (a) air temperature, (b) mean radiant temperature, (c) operative temperature, and (d) numerical specification

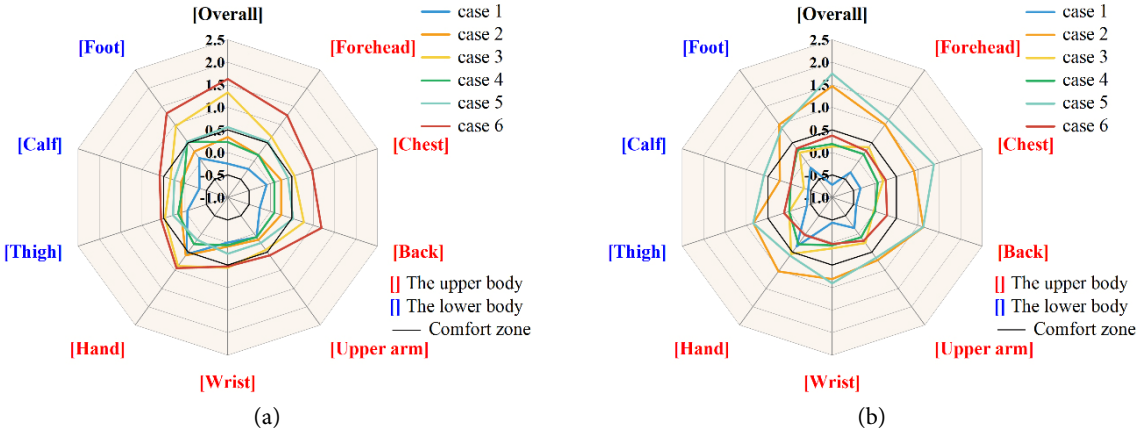

Fig. 6 Human local and overall thermal sensation under different conditions: (a) sunlit zone and (b) shade zone

A comparison of (FC+RF) (Cases 1–3) with FC alone (Cases 4–6) showed that (FC+RF) might improve lower-body comfort. RF addition, especially in the feet area, reduced thermal discomfort by 0.27–0.49 when cooling was activated. Even with reduced operation areas, (FC+RF) maintained comfort, contrasting with FC only setups where the decreased active area caused overall thermal sensation to fall outside the optimal range. (FC+RF) also achieved a more balanced thermal sensation compared to FC alone.

The influence on thermal sensation of activating the

sunlit zone while only using FC was explored (Cases 4 and 5). The partition of the FC activation area in half caused the overall TSV to deviate from the suitable assessment range (−0.5 to +0.5). This notion indicates that the incorporation of RF can significantly expand the load range of the HVAC system to maintain a better indoor thermal environment. By comparing the impact on thermal sensation of activating the shade zone (Cases 3 and 6). The results showed that, (FC+RF) provides a more balanced overall thermal sensation compared with using FC alone. In addition, this study calculated the correlation between upper and lower body thermal sensations and overall thermal sensation for different terminal forms. For (FC+RF), the correlation was 0.894 for the upper body and 0.759 for the lower body. For FC, the correlation was 0.881 for the upper body and 0.618 for the lower body. Comparison of the results showed that the correlation of both end forms with the upper body was relatively strong, exceeding 0.88, while the correlation with the lower body was relatively weak. The correlation between FC and the lower body was significantly lower than (FC+RF), which may be attributed to the greater influence of RF on the lower body.

These results suggest that (FC+RF) systems enhance indoor comfort without solar radiation and offer design insights for effective cooling strategies considering solar loads.

3.3 Difference in environmental parameters between sunlit and shade zones

Considering the influence of solar radiation on the indoor thermal environment, this study conducted Cases 7 to 12 with curtains open to enhance the applicability in real-life scenarios. Figure 7 provides a comparative analysis of the various indoor environmental parameters, including T_a, T_{mrt}, and T_{op}.

In the study, thermal sensations ranged from −1 to 3, with −1 being less common, mostly early in the experiment when the sunlit area was small. Figure 7's box plots show how environmental parameters correspond to thermal

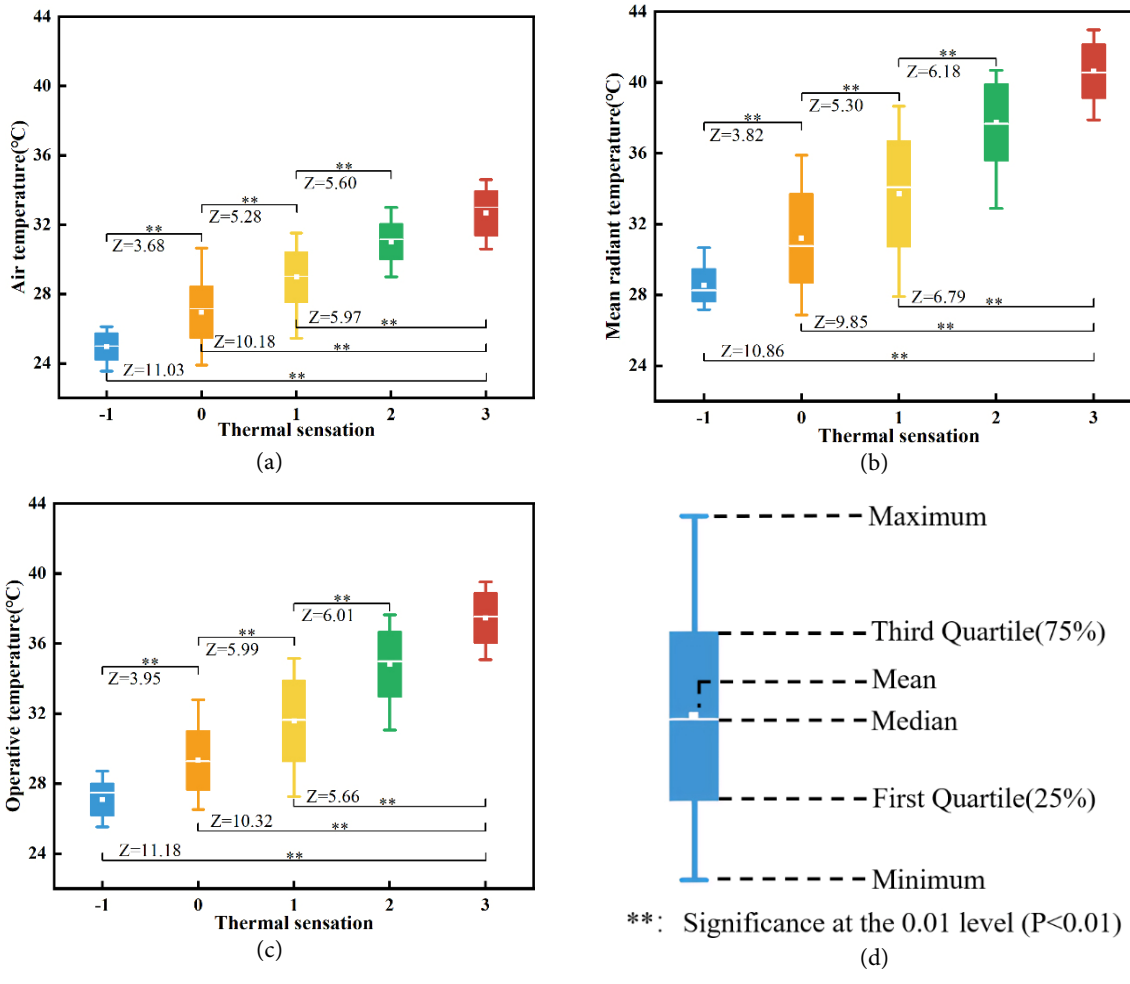

Fig. 7 Interval diagram of the environmental parameters relative to overall thermal sensation under solar irradiation: (a) air temperature, (b) mean radiant temperature, (c) operative temperature, and (d) numerical specification

sensations. Data from five sets under three parameters were analyzed, confirming significant differences in air temperature between adjacent thermal sensations at lower temperatures, but not at higher temperatures (+2 to +3). However, subjects with the same thermal sensation ratings had elevated temperature range thresholds compared to those without solar radiation. This aligned with Chinazzo et al. (2019), indicating sunlight affected thermal perception. Findings suggest that the distinction between +2 and +3 thermal sensations is unclear and not statistically significant.

As *Z*-values rise, the impact of three temperature parameters on thermal sensation intensifies. Solar radiation notably impacted all indoor temperature parameters, with mean radiant temperature (T_{mrt}) and operative temperature (T_{op}) increasing more than air temperature (T_a). Focusing only on T_a's changes didn't fully capture the effects of solar radiation on the indoor environment and occupants. Comparing thermal sensations by the *Z*-values shows T_{op}'s *Z*-value is significantly more relevant and stable than T_a's. This, along with prior analysis, suggests that operative temperature is a more accurate indicator of thermal sensation, even with solar radiation present.

In this section, Cases 7 to 12 were analyzed, which involved the influence of solar radiation on the performance of HVAC systems. The analysis explored how solar heat gain as a variable affected the inherent performance of the system, particularly in the distribution of cold air and the provision of indoor cooling.

Figure 8 displays the outdoor solar radiation intensity on each experimental day of this study. As seen in the figure, the radiation intensity showed significant fluctuations, which were mainly due to different levels of cloud cover during the experiment. Despite the fluctuations, the solar radiation intensity during each experiment exhibited a similar range of variations. It is worth noting that in actual experimental practice, as the azimuth and altitude angles of the sun varied throughout the day, the area of sunlight reaching the human body increased, resulting in a corresponding increase in the amount of solar radiation absorbed by the human body. According to Liu et al.'s research (Liu et al. 2020) and in conjunction with our test data in the preparation phase of the experiment, the irradiance coefficients were set at 0.2, 0.4, and 0.7 for the time intervals of 14:30 to 15:00, 15:00 to 16:00, and 16:00 to 16:30, respectively, to accurately model this time-varying solar radiation effect.

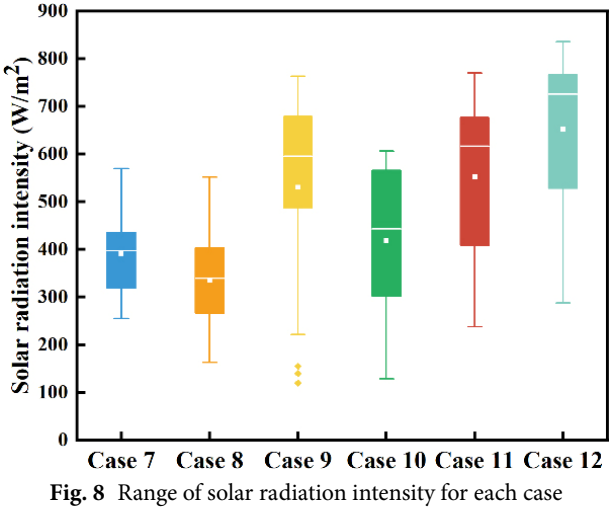

Fig. 8 Range of solar radiation intensity for each case

Figure 9 depicts the changes in local and overall thermal perception experienced by the human body under different conditions: (a) in the sunlit area and (b) in the shaded area. Further analysis compared Cases 7, 8, and 9 (FC+RF) with Cases 10, 11, and 12 (FC). This comparison aimed to assess the additional effects of floor radiation cooling. (FC+RF) may have offered better lower body comfort without generating excessive air movement, which is particularly beneficial for summer cooling.

In sunlit and shaded zones (Cases 7 and 10), (FC+RF) seemed to cool the lower body more evenly, useful during the summer. Only in the sunlit zone (Cases 8 and 11), the sunlit zone needed more cooling. Case 8 stayed near comfort for feet and calves with RF, but the shaded area in Case 11 didn't cool enough with just FC, showing FC's limits in intense conditions. In the shaded zone only (Cases 9 and 12), there was a clear difference in thermal sensation between the two systems. Case 12 had uneven heating, particularly at the head and feet, suggesting FC alone doesn't distribute heat well, which (FC+RF) improved.

The relationship between the thermal sensations of the body's upper and lower parts to the overall feeling was studied under solar radiation effects. With (FC+RF), the upper body correlation was 0.855 and the lower body was 0.723. For FC, it was 0.818 for the upper body and 0.503 for the lower body. Both systems correlated better with the upper body even with solar radiation, but the lower body correlation was weaker. However, the correlation between different body parts and overall thermal sensation showed a decreasing trend due to the involvement of solar radiation, and FC only showed a moderate link for the lower body.

When the aforementioned and previous analyses were integrated, the analysis of indoor thermal comfort under the influence of solar radiation indicated that the cooling capacity of FC was significantly insufficient under adverse conditions of solar radiation. Increasing the temperature difference or airflow to enhance cooling might have resulted in a stronger sensation of draft and discomfort from cold air for indoor occupants and reduced the stability of the indoor environment. By contrast, (FC+RF) could effectively increase the cooling capacity through radiation. In this system, the floor areas heated by direct sunlight and the

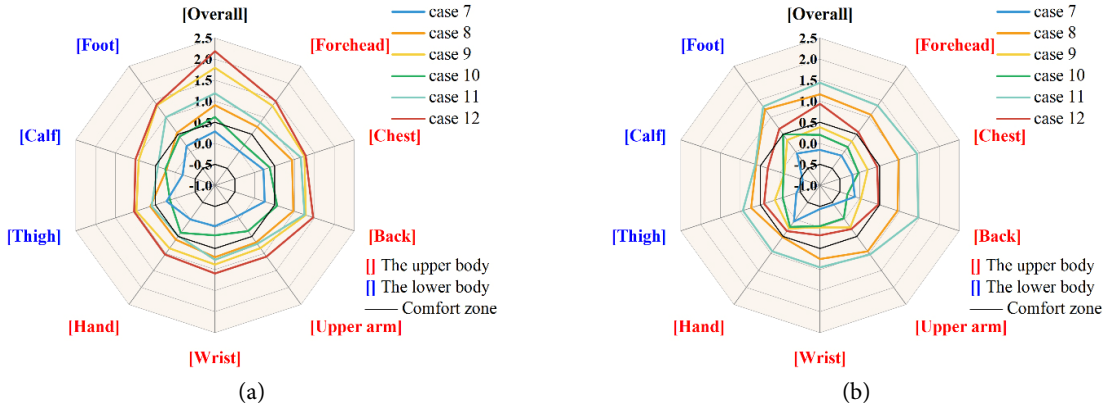

Fig. 9 Human local and overall thermal sensation under different conditions with solar irradiation: (a) sunlit zone and (b) shade zone

surface temperature of the enclosing structures had a more significant effect on indoor occupants. The inclusion of RF could absorb more solar radiation heat at the floor compared with FC and utilize the cold storage properties of the enclosing structures, thereby enhancing indoor thermal comfort and the stability of the indoor environment.

Overall, using (FC+RF) could balance thermal sensation better than FC alone. RF was especially good for the lower body, offering radiant heat from the floor that boosted comfort in warm settings. On the other hand, FC failed to provide enough cooling for the feet, as shown by higher thermal sensation readings. Therefore, the study recommended (FC+RF) in areas needing better lower body cooling, like enclosed spaces or ones with less air movement near the legs, to optimize summer cooling.

As for the impact of sunlight versus shade zones, turning off the air conditioning typically made the upper body feeling hotter, especially the head and chest, key areas for feeling comfortable. In contrast, using (FC+RF) significantly changed lower body sensation, mainly in the legs and feet. This study also pointed out that the activation of a zoned HVAC system significantly affected the thermal sensation in specific areas, such as the open areas within the same indoor space in this experiment, a finding that corroborated current research on personal comfort systems (Udayraj et al. 2018; Yang et al. 2018; Wang et al. 2019; Yang et al. 2022). This notion suggests that implementing a zoned HVAC system might be more effective in areas where people remain stationary for extended periods.

3.4 Relationship between physiological parameters and TSV

3.4.1 Relationship between terminal forms, solar radiation, and T_{skin}

Figure 10 summarizes representative Cases 1, 4, 7, and 10

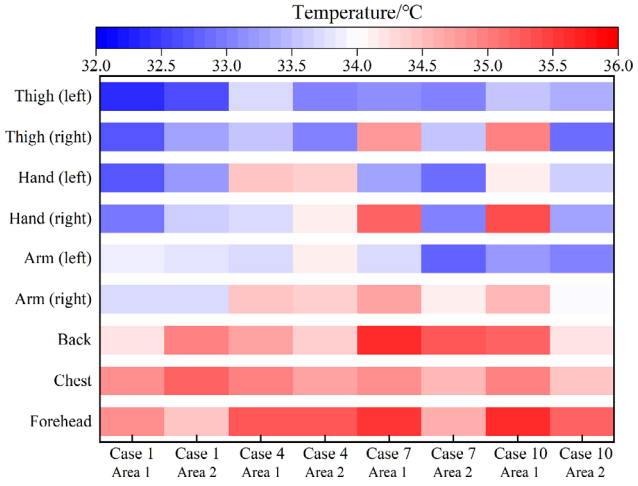

Fig. 10 Local skin temperature in different indoor areas under typical working conditions

from this experiment. Sunlit and shade zones are referred to as Areas 1 and 2, respectively, to avoid ambiguity in this section. These cases covered a range of terminal form settings and exposure to sunlight. Skin temperature readings across different body parts were greatly affected by the HVAC system's status and the presence of sunlight, with the lower body being generally cooler than the upper body. The (FC+RF) system had a notable effect on the lower body, suggesting that adding RF was key in lessening the impact of sunlight on thermal comfort. Comparing Cases 7 and 10, direct sunlight notably raised skin temperature on the body's right side, with increases of 0.79 °C and 0.83 °C under FC and (FC+RF), respectively, sometimes reaching 2.15 °C. Even so, (FC+RF) typically lowered skin temperature more than FC alone. Also, by looking at Cases 1 and 4, we saw (FC+RF) helped equalize local skin temperatures between sunlit and shaded areas, pointing to its ability to make the indoor thermal environment more uniform. There was a notable temperature variation among body parts, whether in a uniform or varying thermal environment, showing that

different body parts contributed unevenly to the overall thermal sensation. This indicates a need to further study how sensitive different parts of the body are to temperature changes.

3.4.2 *Relationship between T_{skin} and TSV*

Figures 11(a) and 11(b) illustrate the correlation between the TSV of the different body parts and the overall TSV, both under conditions without and with solar irradiation, respectively. Figure 11(a) depicts that the upper body, except for the hands, shows a moderate to high positive correlation with the overall TSV ($0.5 < \rho < 1$, $p < 0.05$). The thighs and calves of the lower body also showed a moderate to high positive correlation with the overall TSV ($0.5 < \rho < 0.65$, $p < 0.05$). The TSV of the feet often had the most significant influence on the overall thermal sensation in winter (Wang et al. 2022; Li et al. 2023), yet this differed in summer in this study, potentially because of the insulating effect of sports shoes and cotton socks, as seen in Figures 6 and 9.

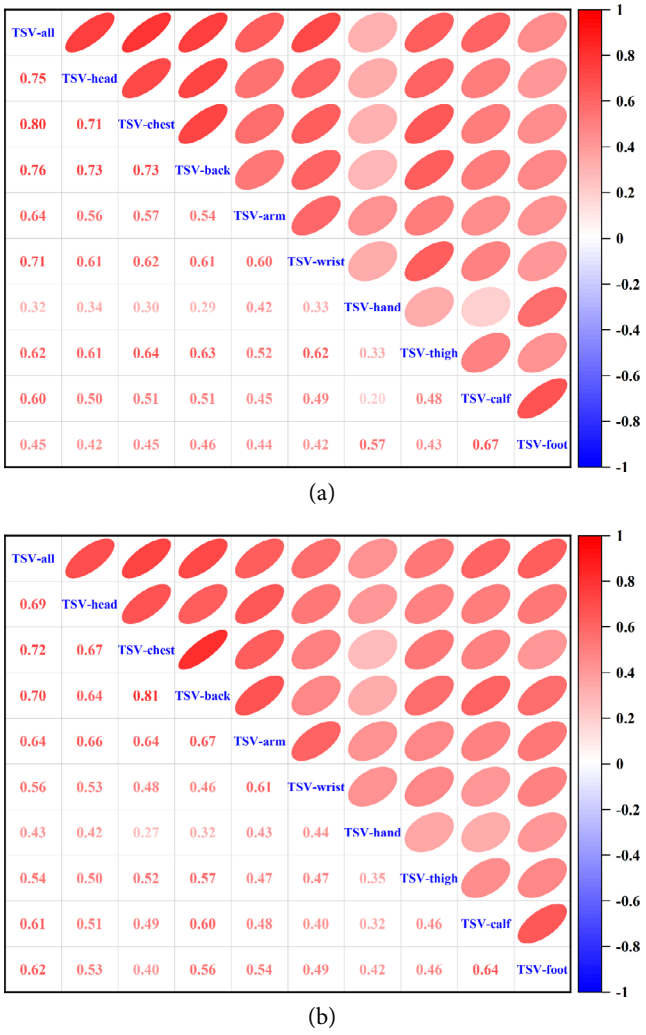

(a)

(b)

Fig. 11 Correlation analysis of the TSV for the human body parts and overall: (a) non-solar radiation and (b) solar radiation

In the analysis of Figure 11(b), the correlation patterns among different body parts are similar to those without solar exposure despite the presence of solar irradiation, with only the foot area showing an increase in correlation from 0.45 to 0.62, indicating a moderate to high positive correlation. The analysis suggests that the intensified thermal sensation in the foot area is due to solar radiation heating the floor and skin. In summary, sunlight didn't drastically change how we perceived our body's thermal comfort. Predicting overall TSV worked for conditions both with and without sunlight. Therefore, to predict thermal sensation in sunny indoor settings, measuring the upper body and average skin temperatures should be given priority.

3.4.3 *Relationship between TSV, blood pressure, and PR*

Choi's study (Choi et al. 2012) delved into the variation in pulse rate (PR) and pointed out that ambient temperature had a significant effect on heart rate: in warm environments, individuals showed a significant increase in heart rate compared to cold conditions. This phenomenon not only demonstrates the close relationship between heart rate and body temperature, but also reflects the ability of the physiological regulatory system to respond sensitively to changes in ambient temperature. Xu et al.'s study revealed the effects of short-term heat exposure on blood pressure and heart rate, which provided a basis for further understanding of how environmental factors affected physiological responses (Xu et al. 2019). Their findings emphasized significant shifts in cardiovascular parameters, specifically systolic blood pressure (SBP), diastolic blood pressure (DBP), and PR, in response to changes in heat perception.

In Figure 12, a gradual increase in SBP and DBP could be observed as the sensation shifted from cold to hot, further emphasizing the direct link between thermal comfort and cardiovascular stress. This finding revealed a possible point of monitoring and intervention, especially in contexts where hot environments might pose a threat to an individual's health. In addition, by comparing Figures 12(a) and (b), it could be observed that the PR increased significantly at higher levels of thermal sensation, suggesting that the cardiovascular system's response to heat stress might intensify with increasing temperature. The discovery of this pattern was critical for understanding how the cardiovascular system adjusts to transient environmental changes and may inform the development of protective measures for staff working in hot environments. However, while these results provide some insight, detailed mechanisms on how heat exposure specifically affects cardiovascular function still require more detailed study.

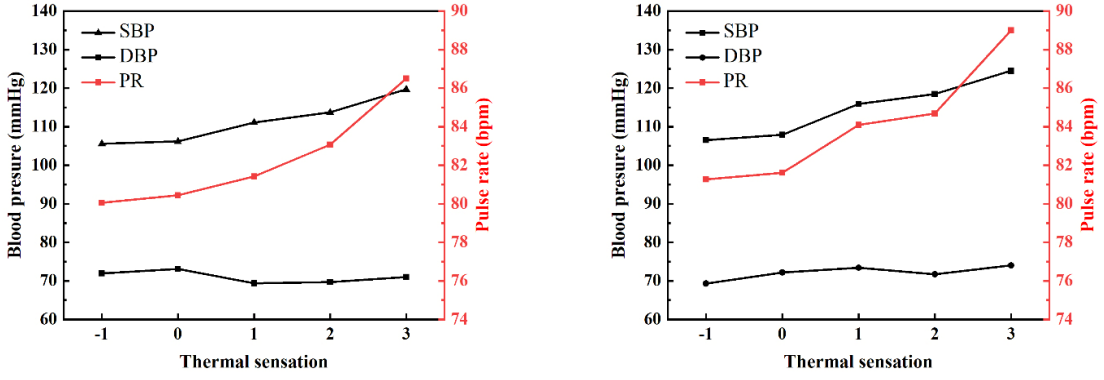

Fig. 12 Interval diagram of blood pressure and heart rate relative to thermal sensation: (a) non-solar radiation and (b) solar radiation

4 Discussion

4.1 Relationship between T_{op} and T_{skin}

Among the various physiological parameters, T_{skin} was often used to predict the TSV of indoor occupants due to its numerous measurement points, wide coverage of the human body, and high accuracy (Wang et al. 2015; Choi and Yeom 2017; Wu et al. 2019; Liu et al. 2022a; Pan et al. 2022; Wang et al. 2022). However, the high accuracy of skin temperature measurements often implies a more cumbersome process. Currently, the common methods of temperature measurement are divided into contact and non-contact types, with non-contact methods, such as infrared thermometry, are more convenient but ineffective for areas covered by clothing, whereas contact thermometry, although more precise, is even more laborious. This study attempted to analyze the relationship between T_{op} and T_{skin} by integrating the above analysis, which identified a significant correlation between T_{op} and TSV. In electrophysiological research, an S-shaped expression function—the Boltzmann equation—was often used to reflect certain physiological regulatory characteristics of the human body (Li et al. 2019). Based on the aforementioned average T_{skin} for the corresponding temperature intervals, performing Boltzmann regression fitting on T_{op} and T_{skin} yielded a characteristic curve of T_{skin} variations with T_{op} (Figure 13).

The regression models for conditions without and with solar irradiation are shown in Equations (5) and (6), respectively. The adjusted R^2 values of the two models are 0.94 and 0.97, indicating a good fit and accurate reflection of the variation patterns of skin temperature at measurement points with environmental parameters.

$$y = 34.90 - \frac{1.55}{1 + e^{(T_{op} - 27.38)/0.69}} \quad (R^2 = 0.94) \tag{5}$$

$$y = 36.39 - \frac{3.8}{1 + e^{(T_{op} - 28.51)/4.13}} \quad (R^2 = 0.97) \tag{6}$$

The model showed that the T_{skin} variation range in this study spanned from 33.21 °C to 35.03 °C and from 33.91 °C to 36.15 °C. When T_{op} varied within the neutral temperature range, T_{skin} increased almost linearly with the rise in environmental parameters. However, an inflection or slowing trend in the body's skin temperature was observed when the environmental temperature rose to a certain stage, this was consistent with the findings of Xiong et al. (2015), who also reported changes in the body's thermoregulatory mechanisms and an enhanced heat stress response after a certain ambient temperature phase. In hotter environments (blue dashed line in Figure 13), T_{skin} fluctuated around 36 °C with the increase in environmental T_{op}, indicating strong thermal stress responses in the body due to the ambient temperature. This was similar to the observations of Kenny and Flouris (2014) under similar conditions. They noted that when the ambient temperature increases to the upper limit of the regulatory capacity of the body's

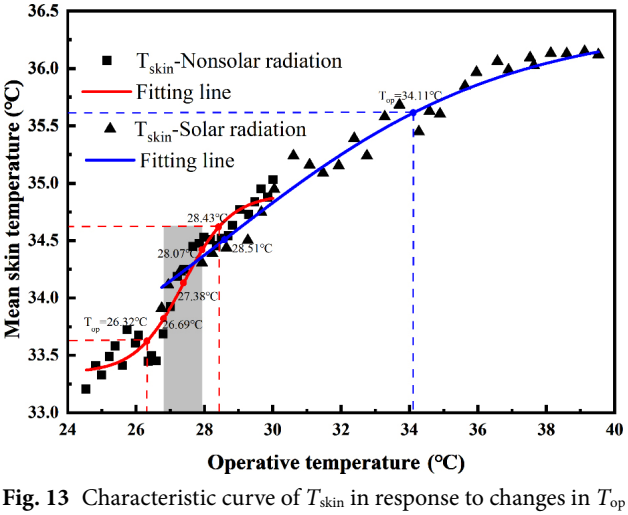

Fig. 13 Characteristic curve of T_{skin} in response to changes in T_{op}

thermoregulatory system, the body responded by increasing heat dissipation mechanisms, such as sweating, but this regulatory capacity was limited. This was supported in our study and was in line with the findings of Henderson and Halsey (2022), who observed an increase in physiological stress in the body under conditions of heat stress and its potential impact on work efficiency and health. Prolonged exposure to such environments can increase physiological strain, significantly impaired work efficiency, and may even result in physiological damage, affecting health.

MATLAB was used to perform first derivative, second derivative, and inverse function calculations on Equations (5) and (6) to explore the sensitive ranges of environmental parameters for the two models. The maximum slopes of the two models were found to be 0.56 and 0.23, corresponding to T_{op} of 27.38 °C and 28.51 °C, respectively. Based on the extremum properties of the functions, the significant T_{op} range for T_{skin} variation in Equation (5) was identified as 26.69 °C to 28.07 °C. This notion indicates that the human skin temperature has the highest response rate to changes in environmental parameters within this range, suggesting the greatest physiological regulatory capacity in this temperature interval. Subsequent calculations of the curvature equations and first derivative and inverse function operations were performed to locate the extreme points of the curvature functions of the two models, namely, the points where the slope of the curvature function is zero, yielding the corresponding operative temperatures for Equation (5) at its extremal points as 26.32 °C and 28.43 °C, while it was 34.11 °C for Equation (6). This notion indicates that in Equation (5), T_{skin} started to show a turning point in the range of 26.32 °C to 28.43 °C, becoming less sensitive to temperature adjustments. In Equation (6), a turning point occurred in the range of 28.51 °C to 34.11 °C, showing decreased sensitivity to temperature changes. When T_{op} exceeds 34.11 °C, surpassing the normal physiological regulation capacity of the human body, mechanisms, such as excessive sweating, occur to maintain a stable skin temperature, to which this model was not sensitive.

4.2 Relationship between T_{skin} and TSV

This study also conducted linear fitting of TSV and T_{skin} for participants under conditions with and without solar irradiation. The results are shown in Figure 14. The regression models for conditions without and with solar irradiation are presented in Equations (7) and (8), respectively. The adjusted R^2 values for both models are 0.92 and 0.94, indicating a good fit and accurately reflecting the variation patterns between T_{skin} and TSV. It could be found that the thermal sensation vote (TSV) values of sun-exposed

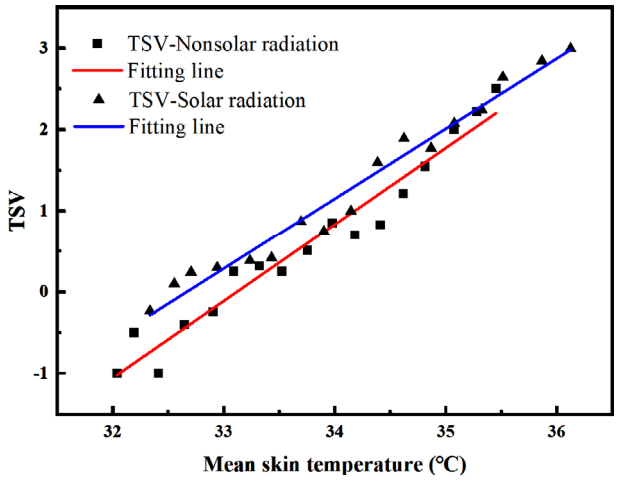

Fig. 14 Response characteristic curve of the TSV with changes in T_{skin}

participants were higher than those of non-exposed participants, even under the same environmental conditions, with an average increase in TSV values of about 0.2 to 0.5, suggesting that the human body is more sensitive to thermal perception in the vicinity of the comfort zone when exposed to the sun. This finding was consistent with the findings by La Gennusa et al. (2007) and Ning et al. (2023), who noted that solar radiation significantly increased the perceived temperature of the human body, which in turn affected comfort perception. Their work demonstrated that the effects of solar radiation can make the body feel hotter even when the ambient temperature remains constant, which was consistent with the increase in TSV observed in our study under sun-exposed conditions. Similarly Pan et al. (2022) observed in their study, through a controlled laboratory setup and field survey, that direct sunlight caused subjects to report higher heat perception, especially when they were in the comfort zone of the temperature, which further supports our finding that sun exposure could increase heat perception, especially when the temperature was close to the comfort zone.

Taken together, these results suggest that solar irradiation is an important factor in thermal comfort perception and needs to be considered when designing and evaluating indoor and outdoor environments.

$$y = 0.94T_{skin} - 31.23 \quad (R^2 = 0.92) \quad (7)$$

$$y = 0.86T_{skin} - 28.18 \quad (R^2 = 0.94) \quad (8)$$

4.3 Limitations and further research

This study provides a preliminary investigation of the effect of solar radiation on the thermal sensation of indoor occupants under convection–radiation cooling systems

conditions, simplifying the process of predicting thermal comfort and reduce the complexity of incorporating psychological factors into the prediction. It should be noted, however, that since the study was conducted under specific conditions and with a specific population, this may limit the broad applicability of the conclusions obtained. Future studies need to be conducted in a wider range of environments and populations to deepen our understanding of how solar radiation affects human thermal sensation.

5 Conclusion

This study investigated the changes in physiological and psychological responses to the presence or absence of solar radiation in different terminal forms and indoor areas through experimental methods combining environmental and physiological parameters with subjective questionnaires under various terminal forms and indoor area conditions. The operative temperature T_{op} was used to fit the mean skin temperature T_{skin}, providing a model to predict human physiological parameters using environmental parameters under specific conditions. The main findings of this study can be summarized as follows:

1) Temperature parameters are the primary factors influencing thermal sensation. The comparison of the standard-test-statistical Z values indicates that operative temperature is a more effective indicator for judging thermal sensation.

2) Different forms of terminals produce different levels of comfort, with (FC+RF) providing greater lower-body comfort (with a correlation coefficient of 0.723) than FC (with a correlation coefficient of 0.503) in summer conditions.

3) Solar radiation reduces the possibility of achieving indoor thermal comfort. Compared to FC, radiant cooling in (FC+RF) can be utilized to improve thermal comfort and stabilize the indoor environment by absorbing solar heat from the floor when exposed to direct sunlight.

4) Prediction of thermal sensation under solar radiation should focus on the upper body and mean skin temperatures.

5) A fitting model has been established for T_{op} and T_{skin} under conditions without and with solar radiation. The sensitive ranges of the two models were determined through mathematical analysis to be between 26.32 °C and 28.43 °C, and 28.51 °C and 34.11 °C, respectively.

Acknowledgements

This work was supported by the Open Fund (No. 202303 and No. 202304) of the Sichuan Province Engineering Technology Research Center of Healthy Human Settlement and Key R&D Plan of Sichuan Science and Technology Program (No. 2022YFG0138-LH).

Declaration of competing interest

The authors have no competing interests to declare that are relevant to the content of this article.

Author contribution statement

Guanyu Li: experimental test, writing–original draft, and editing. Dong Liu: writing—original draft, review and supervision. Anjie Hu: review and editing. Qidong Yan: acquisition and analysis of data. Lina Ma: experimental test. Liu Tang: supervision. Xiaozhou Wu: supervision. Jun Wang: supervision. Zhenyu Wang: supervision. All authors read and approved the final manuscript.

References

A Y, Li N, He Y, et al. (2022). Occupant-centered evaluation on indoor environments and energy savings of radiant cooling systems with high-intensity solar radiation. *Solar Energy*, 242: 30–44.

Atlas Weather (2023). Mianyang climate—Mianyang temperatures–best travel time–weather. Available at https://www.weather-atlas.com/zh/china/mianyang-climate.

Chaiyapinunt S, Khamporn N (2021). Effect of solar radiation on human thermal comfort in a tropical climate. *Indoor and Built Environment*, 30: 391–410.

Chinazzo G, Wienold J, Andersen M (2019). Daylight affects human thermal perception. *Scientific Reports*, 9: 13690.

Choi JH, Loftness V, Lee DW (2012). Investigation of the possibility of the use of heart rate as a human factor for thermal sensation models. *Building and Environment*, 50: 165–175.

Choi JH, Yeom D (2017). Study of data-driven thermal sensation prediction model as a function of local body skin temperatures in a built environment. *Building and Environment*, 121: 130–147.

Choi JK, Miki K, Sagawa S, et al. (1997). Evaluation of mean skin temperature formulas by infrared thermography. *International Journal of Biometeorology*, 41: 68–75.

Cohen J (1992). Quantitative methods in psychology: A power primer. *Psychological Bulletin*, 112: 155–159.

Djongyang N, Tchinda R, Njomo D (2010). Thermal comfort: A review paper. *Renewable and Sustainable Energy Reviews*, 14: 2626–2640.

Fang Z, Feng X, Lin Z (2017). Investigation of PMV Model for Evaluation of the Outdoor Thermal Comfort. *Procedia Engineering*, 205: 2457–2462.

Fanger PO (1970). Thermal Comfort: Analysis and Applications in Environmental Engineering. Copenhagen, Denmark: Danish Technical Press.

Golmohammadi R, Yousefi H, Safarpour Khotbesara N, et al. (2021). Effects of light on attention and reaction time: A systematic review. *Journal of Research in Health Sciences*, 21: e00529.

Henderson MET, Halsey LG (2022). The metabolic upper critical temperature of the human thermoneutral zone. *Journal of Thermal Biology*, 110: 103380.

Hodder SG, Parsons K (2007). The effects of solar radiation on thermal comfort. *International Journal of Biometeorology*, 51: 233–250.

Huang L, Kang J (2021). Thermal comfort in winter incorporating solar radiation effects at high altitudes and performance of improved passive solar design—Case of Lhasa. *Building Simulation*, 14: 1633–1650.

ISO 7726 (2002). Ergonomics of the Thermal Environment—Instruments for Measuring Physical Quantities. International Standardization Organization, Geneva.

Ji Y, Liu G, Zhang Y, et al. (2024). Effects of the clothing colors on heat transfer and thermal sensation under indoor solar radiation in winter. *Case Studies in Thermal Engineering*, 53: 103899.

Kenny GP, Flouris AD (2014). The human thermoregulatory system and its response to thermal stress. In: Wang F, Gao C (eds), Protective Clothing: Managing Thermal Stress. Cambridge, UK: Woodhead Publishing, pp. 319–365.

Kim S, Ryu J, Seo H, et al. (2022). Understanding occupants' thermal sensitivity according to solar radiation in an office building with glass curtain wall structure. *Buildings*, 12: 58.

Kolarik J, Toftum J, Olesen BW, et al. (2011). Simulation of energy use, human thermal comfort and office work performance in buildings with moderately drifting operative temperatures. *Energy and Buildings*, 43: 2988–2997.

La Gennusa M, Nucara A, Rizzo G, et al. (2005). The calculation of the mean radiant temperature of a subject exposed to the solar radiation—A generalised algorithm. *Building and Environment*, 40: 367–375.

La Gennusa M, Nucara A, Pietrafesa M, et al. (2007). A model for managing and evaluating solar radiation for indoor thermal comfort. *Solar Energy*, 81: 594–606.

Lan L, Lian Z (2010). Application of statistical power analysis—How to determine the right sample size in human health, comfort and productivity research. *Building and Environment*, 45: 1202–1213.

Lei TH, Lan L, Wang F (2023). Indoor thermal comfort research using human participants: Guidelines and a checklist for experimental design. *Journal of Thermal Biology*, 113: 103506.

Leung C, Ge H (2013). Sleep thermal comfort and the energy saving potential due to reduced indoor operative temperature during sleep. *Building and Environment*, 59: 91–98.

Li B, Li W, Liu H, et al. (2010). Physiological expression of human thermal comfort to indoor operative temperature in the non-HVAC environment. *Indoor and Built Environment*, 19: 221–229.

Li B, Du C, Liu H, et al. (2019). Regulation of sensory nerve conduction velocity of human bodies responding to annual temperature variations in natural environments. *Indoor Air*, 29: 308–319.

Li Z, Zhang D, Li C (2021). Experimental evaluation of indoor thermal environment with modularity radiant heating in low energy buildings. *International Journal of Refrigeration*, 123: 159–168.

Li Q, Liu H, Wu Y, et al. (2023). Effects of constant and fluctuating temperature modes of foot heating on human thermal responses in cold environments. *Building and Environment*, 238: 110364.

Liang Y, Zhang N, Wu H, et al. (2021). Thermal environment and thermal comfort built by decoupled radiant cooling units with low radiant cooling temperature. *Building and Environment*, 206: 108342.

Liu X, Gong G, Cheng H, et al. (2012). Airflow and heat transfer in the slot-vented room with radiant floor heating unit. *Journal of Applied Mathematics*, 2012: 287271.

Liu G, Wang Z, Li C, et al. (2020). Heat exchange character and thermal comfort of young people in the building with solar radiation in winter. *Building and Environment*, 179: 106937.

Liu D, Liu N, Ren D, et al. (2022a). The thermal responses between young adults and preschool children in a radiant floor heating environment. *Buildings*, 12: 2234.

Liu D, Zhou H, Hu A, et al. (2022b). Study on the intermittent operation mode characteristic of a convection–radiation combined cooling system in office buildings. *Energy and Buildings*, 255: 111669.

Liu D, Li G, Wu X, et al. (2023). Comparative analysis of heating characteristics of convective-radiant systems using various terminal air source heat pumps. *Energy and Buildings*, 301: 113701.

Liu Q, Li N, He Y, et al. (2024). Quantifying the effects of indoor non-uniform solar radiation on human thermal comfort and work performance in warm season. *Energy and Buildings*, 306: 113962.

Marino C, Nucara A, Pietrafesa M (2015). Mapping of the indoor comfort conditions considering the effect of solar radiation. *Solar Energy*, 113: 63–77.

Marino C, Nucara A, Pietrafesa M (2017a). Thermal comfort in indoor environment: Effect of the solar radiation on the radiant temperature asymmetry. *Solar Energy*, 144: 295–309.

Marino C, Nucara A, Pietrafesa M, et al. (2017b). The effect of the short wave radiation and its reflected components on the mean radiant temperature: Modelling and preliminary experimental results. *Journal of Building Engineering*, 9: 42–51.

McIntyre DA, Griffiths IS (1972). Radiant temperature and thermal comfort. In: Symposium of Thermal Comfort and Moderate Heat Stress. Kanata, ON, Canada: CIB Commission, Working Commission 45.

McNall PE, Schlegel JC (1968). The relative effects of convection and radiation heat transfer on thermal comfort (thermal neutrality) for sedentary and active human subjects. *ASHRAE Transactions*, 74: 131–142.

Mollon JD, Bosten JM, Peterzell DH, et al. (2017). Individual differences in visual science: What can be learned and what is good experimental practice? *Vision Research*, 141: 4–15.

Ning S, Jing W, Ge Z (2023). Sunlight perception and outdoor thermal comfort in college campuses: A new perspective. *Scientific Reports*, 13: 16112.

Pan J, Li N, Zhang W, et al. (2022). Investigation based on physiological parameters of human thermal sensation and comfort zone on indoor solar radiation conditions in summer. *Building and Environment*, 226: 109780.

Singh MC, Garg SN (2011). Suitable glazing selection for glass-curtain walls in tropical climates of India. *ISRN Renewable Energy*, 2011: 484893.

Somasundaram S, Chong A, Wei Z, et al. (2020). Energy saving potential of low-e coating based retrofit double glazing for tropical climate. *Energy and Buildings*, 206: 109570.

Song B, Bai L, Yang L (2022). Analysis of the long-term effects of solar radiation on the indoor thermal comfort in office buildings. *Energy*, 247: 123499.

Udayraj, Li Z, Ke Y, et al. (2018). A study of thermal comfort enhancement using three energy-efficient personalized heating strategies at two low indoor temperatures. *Building and Environment*, 143: 1–14.

Vadiee A, Dodoo A, Jalilzadehazhari E (2019). Heat supply comparison in a single-family house with radiator and floor heating systems. *Buildings*, 10: 5.

Wang Y, Liu Y, Song C, et al. (2015). Appropriate indoor operative temperature and bedding micro climate temperature that satisfies the requirements of sleep thermal comfort. *Building and Environment*, 92: 20–29.

Wang L, Tian Y, Kim J, et al. (2019). The key local segments of human body for personalized heating and cooling. *Journal of Thermal Biology*, 81: 118–127.

Wang H, Wang J, Li W, et al. (2022). Experimental study on a radiant leg warmer to improve thermal comfort of office workers in winter. *Building and Environment*, 207: 108461.

Wu Y, Liu H, Li B, et al. (2019). Thermal adaptation of the elderly during summer in a hot humid area: Psychological, behavioral, and physiological responses. *Energy and Buildings*, 203: 109450.

Xie X, Xia F, Zhao Y, et al. (2022). Parametric study on the effect of radiant heating system on indoor thermal comfort with/without external thermal disturbance. *Energy*, 249: 123708.

Xiong J, Lian Z, Zhou X, et al. (2015). Effects of temperature steps on human health and thermal comfort. *Building and Environment*, 94: 144–154.

Xu D, Zhang Y, Wang B, et al. (2019). Acute effects of temperature exposure on blood pressure: An hourly level panel study. *Environment International*, 124: 493–500.

Yang L, Yan H, Lam JC (2014). Thermal comfort and building energy consumption implications—A review. *Applied Energy*, 115: 164–173.

Yang H, Cao B, Zhu Y (2018). Study on the effects of chair heating in cold indoor environments from the perspective of local thermal sensation. *Energy and Buildings*, 180: 16–28.

Yang B, Wu M, Li Z, et al. (2022). Thermal comfort and energy savings of personal comfort systems in low temperature office: A field study. *Energy and Buildings*, 270: 112276.

Yi L, Xie Y, Lin C (2022). Thermal environment and energy performance of a typical classroom building in a hot-humid region: A case study in Guangzhou, China. *Geofluids*, 2022: 3226001.

Zhou X, Liu Y, Zhang J, et al. (2022). Radiant asymmetric thermal comfort evaluation for floor cooling system—A field study in office building. *Energy and Buildings*, 260: 111917.